Cell

# Multimodal Integration of Carbon Dioxide and Other Sensory Cues Drives Mosquito Attraction to Humans

Conor J. McMeniman,[1] Román A. Corfas,[1] Benjamin J. Matthews,[1] Scott A. Ritchie,[2] and Leslie B. Vosshall[1,3,*]
[1]Laboratory of Neurogenetics and Behavior, The Rockefeller University, New York, NY 10065, USA
[2]School of Public Health, Tropical Medicine and Rehabilitative Sciences, James Cook University, Cairns, QLD 4870, Australia
[3]Howard Hughes Medical Institute
*Correspondence: leslie.vosshall@rockefeller.edu
http://dx.doi.org/10.1016/j.cell.2013.12.044

## SUMMARY

Multiple sensory cues emanating from humans are thought to guide blood-feeding female mosquitoes to a host. To determine the relative contribution of carbon dioxide ($CO_2$) detection to mosquito host-seeking behavior, we mutated the *AaegGr3* gene, a subunit of the heteromeric $CO_2$ receptor in *Aedes aegypti* mosquitoes. *Gr3* mutants lack electrophysiological and behavioral responses to $CO_2$. These mutants also fail to show $CO_2$-evoked responses to heat and lactic acid, a human-derived attractant, suggesting that $CO_2$ can gate responses to other sensory stimuli. Whereas attraction of *Gr3* mutants to live humans in a large semi-field environment was only slightly impaired, responses to an animal host were greatly reduced in a spatial-scale-dependent manner. Synergistic integration of heat and odor cues likely drive host-seeking behavior in the absence of $CO_2$ detection. We reveal a networked series of interactions by which multimodal integration of $CO_2$, human odor, and heat orchestrates mosquito attraction to humans.

## INTRODUCTION

Anthropophilic female mosquitoes possess a strong innate drive to find and blood-feed on humans, whose blood provides a protein source needed for egg development. As a consequence of such host-seeking behavior, many mosquito species including the yellow fever mosquito *Aedes aegypti* and the African malaria mosquito *Anopheles gambiae* efficiently spread blood-borne diseases such as dengue and malaria between humans. To orient toward hosts, female mosquitoes detect a variety of chemical and physical cues including body odor, $CO_2$, moisture, heat, and visual contrast (reviewed in Gibson and Torr, 1999). Of these sensory cues, the ~4% $CO_2$ exhaled in breath is a potent behavioral activator and attractant for mosquitoes and is often considered to be the most important sensory cue used by these disease vectors to find humans (Gillies, 1980).

In a broad range of mosquito species, $CO_2$ elicits a suite of context-dependent effects (reviewed in Gillies, 1980) that are thought to promote host-seeking behavior. Exposure to $CO_2$ alone strongly activates mosquito flight, increasing the probability of flight take-off and locomotor activity in the absence of directional air currents (Eiras and Jepson, 1991). Filamentous intermittent plumes of $CO_2$ (Dekker et al., 2005; Geier et al., 1999; Healy and Copland, 1995) elicit stereotyped and sustained patterns of upwind flight toward the $CO_2$ source (Dekker and Cardé, 2011).

In *Ae. aegypti*, $CO_2$ increases both the kinetics and fidelity of flight responses to host odor plumes, thereby enhancing source finding (Dekker and Cardé, 2011; Dekker et al., 2005). Several studies have also shown that $CO_2$ enhances mosquito attraction to warmth (Burgess, 1959; Kröber et al., 2010; Maekawa et al., 2011). Despite earlier attempts to quantify the overall effect of exhaled $CO_2$ from breath on attraction to live humans (Snow, 1970), the scale over which $CO_2$ acts and its relative importance compared to all the other sensory cues encountered during mosquito orientation toward a live host remain unclear.

*Ae. aegypti* maxillary palps house a specialized class of olfactory sensory neurons (OSNs) that are exquisitely sensitive to changes in $CO_2$ concentration (Grant et al., 1995). In the vinegar fly *Drosophila melanogaster*, two gustatory receptors (*DmelGr21a* and *DmelGr63a*) function together to mediate $CO_2$ detection (Jones et al., 2007; Kwon et al., 2007). Direct orthologs of *DmelGr21a* and *DmelGr63a* have been identified in a wide range of insect species including *Ae. aegypti*, where they are named *Gr1* and *Gr3*, respectively (Robertson and Kent, 2009). In most non-*Drosophila* insect species examined, a *Gr1* paralog named *Gr2* is present (Figure 1A). Functional studies of *An. gambiae Gr1*, *Gr2*, and *Gr3* orthologs using heterologous expression in *Drosophila* (Lu et al., 2007) and transient knockdown studies in *Ae. aegypti* (Erdelyan et al., 2012) have suggested a conserved role for these genes as candidate $CO_2$ receptors, but the functional requirement of one or more subunits for mosquito $CO_2$ detection is unknown.

Here we used genome editing to engineer *Ae. aegypti* unable to sense $CO_2$, allowing us to uncover the relative contribution of $CO_2$ detection to mosquito host-seeking behavior. We find that attraction to heat and lactic acid are absent in *Gr3* mutants, suggesting that $CO_2$ detection gates responses to these other

sensory cues. Despite these dramatic deficits, *Gr3* mutants show only mild impairment in their attraction to live human subjects in semi-field conditions. Using live animals, we demonstrate that effects of $CO_2$ detection on mosquito host-seeking behavior are dependent on spatial scale. We further provide compelling evidence that mosquito attraction to humans and blood-feeding behavior are driven by multimodal integration of $CO_2$ and other host sensory cues.

## RESULTS

### Generation of Targeted Mutations in *Gr3*

Of the three *Ae. aegypti* $CO_2$ receptors (Figure 1A), we chose to mutate *Gr3* because mutations in the fly ortholog, *DmelGr63a*, were sufficient to disrupt $CO_2$ reception (Jones et al., 2007). We generated null mutations in this gene by injecting a zinc-finger nuclease (ZFN) pair targeting exon 3 of *Gr3* (Figure 1B) into preblastoderm stage mosquito embryos. Two independent *Gr3* alleles were isolated and characterized, $Gr3^{4}$ and $Gr3^{ECFP}$. $Gr3^{4}$ harbors a 4 bp deletion in exon 3 generated by nonhomologous end-joining (Figure 1C), leading to a frameshift and multiple nonsense mutations. We also generated a homologous recombination allele $Gr3^{ECFP}$ (Figure 1D) by coinjecting a donor plasmid for homology-directed repair along with the ZFN mRNAs. In this allele, 33 bp of exon 3 were deleted, and a 2.45 kb cassette was inserted via ZFN-mediated homologous recombination. This insertion marked mutants visually with enhanced cyan fluorescent protein (*ECFP*) fluorescence (Figure 1E) and could be detected in the *Gr3* locus by PCR (Figure 1F). After outcrossing each isolated allele to wild-type mosquitoes for at least five generations, we established heterozygous ($Gr3^{4/+}$ and $Gr3^{ECFP/+}$), homozygous ($Gr3^{4/4}$ and $Gr3^{ECFP/ECFP}$), and heteroallelic ($Gr3^{ECFP/4}$) mutant lines for behavioral characterization.

### *Gr3* Mutants Cannot Sense or Respond Behaviorally to $CO_2$

$CO_2$ is detected by OSNs of large-spiking amplitude that are housed within capitate peg sensilla on the *Ae. aegypti* maxillary palp, along with a small-spiking neuron responsive to 1-octen-3-ol and a third neuron of unknown ligand specificity (Figure 1G) (Grant et al., 1995; McIver, 1972). Previous studies in *An. gambiae* demonstrated that *Gr1*, *Gr2*, and *Gr3* are coexpressed in the $CO_2$-responsive OSN, and *Or8*/*orco* are coexpressed in the 1-octen-3-ol-responsive OSN (Jones et al., 2007; Lu et al., 2007) (Figure 1G). The organization and function of these OSNs are believed to be conserved in *Ae. aegypti* (Bohbot et al., 2007). To determine whether *Gr3* mutants could sense $CO_2$, we performed extracellular recordings of $CO_2$-evoked activity from female capitate peg sensilla using single sensillum electrophysiology. Wild-type and heterozygous female mosquitoes responded robustly to a 1 s pulse of 0.5% $CO_2$, whereas homozygous and heteroallelic mutants were totally unresponsive (Figure 1H). In the mutants, this lack of a $CO_2$-evoked response was accompanied by the complete absence of spontaneous activity in this neuron. In contrast, the 1-octen-3-ol-sensitive cell of all genotypes responded similarly to a 1 s pulse of $10^{-6}$ (R)-1-octen-3-ol (Figure 1I), indicating that our extracellular recordings were targeted correctly to capitate peg sensilla. Summary data showing spontaneous and stimulus-evoked activity are in Figure 1J.

To test whether $CO_2$-evoked behavior was affected in these mutants, we tracked the flying activity of groups of female mosquitoes using 3D multi-insect tracking in a large assay chamber. Following a period of baseline tracking, we introduced a pulse of $CO_2$ into the airstream, which caused large bursts of flight activity in wild-type and heterozygous female mosquitoes (Figures 2A–2C; top three rows). In contrast, homozygous and heteroallelic mutant mosquitoes remained indifferent to this stimulus (Figures 2A–2C; bottom three rows).

To rule out nonspecific locomotor defects in *Gr3* mutants, we tracked the activity of wild-type mosquitoes and a representative homozygous mutant genotype, $Gr3^{ECFP/ECFP}$, over a 23 hr period. No significant differences in either flying distance tracked per mosquito or flight velocity were observed between genotypes, and their daily rhythms of activity were qualitatively similar (Figures 2D and 2E). We conclude that *Gr3* mutants are selectively impaired in their response to $CO_2$.

### $CO_2$ Detection Can Gate Mosquito Heat-Seeking Behavior

Warm-blooded hosts provide mosquitoes with thermal contrast that facilitates the localization of a suitable blood meal. To investigate the potential for an interaction between $CO_2$ detection and heat perception, we developed a heat-seeking assay that scored the ability of mosquitoes to land on a 37°C target (Figures 3A–3C). Trials with wild-type females revealed that mosquitoes only landed on the heated target when a pulse of $CO_2$ was presented in the assay (Figures 3D–3F). Wild-type males were not attracted using identical assay conditions (Figure 3G), showing that heat seeking stimulated by $CO_2$ is sexually dimorphic in *Ae. aegypti*.

To further verify that $CO_2$ detection was required for heat-seeking behavior in female *Ae. aegypti*, we tested the heterozygous, homozygous, and heteroallelic *Gr3* mutants in the same assay. Heterozygous genotypes landed on the heated target in a $CO_2$-dependent manner (Figures 3H and 3I), but homozygous and heteroallelic *Gr3* mutants did not land (Figures 3J–3L), indicating that $CO_2$ detection is required for this behavior. Heat-seeking data are summarized in Figures 3M and 3N.

### $CO_2$ Detection Enhances Mosquito Attraction to Lactic Acid and Human Scent

In addition to exhaled $CO_2$, humans emit a blend of hundreds of volatile organic compounds in breath and skin odor (Gallagher et al., 2008). To evaluate whether $CO_2$ detection influences the ability of *Ae. aegypti* to orient toward human odorants, we used a two-port olfactometer to assay attraction of wild-type, heterozygous, and homozygous *Gr3* mutant female mosquitoes to various odor stimuli in the presence or absence of supplemental $CO_2$ (Figure 4A). After characterizing background levels of attraction using blank trials that contained no stimuli (Figure 4B), we evaluated responses to $CO_2$. We observed moderate numbers of wild-type and heterozygous *Gr3* females trapped in response to stimulation with $CO_2$ alone. However, attraction appeared to be nondirectional with respect to the $CO_2$ source in this assay (Figure 4C, $Gr3^{+/+}$ and $Gr3^{ECFP/+}$). This general

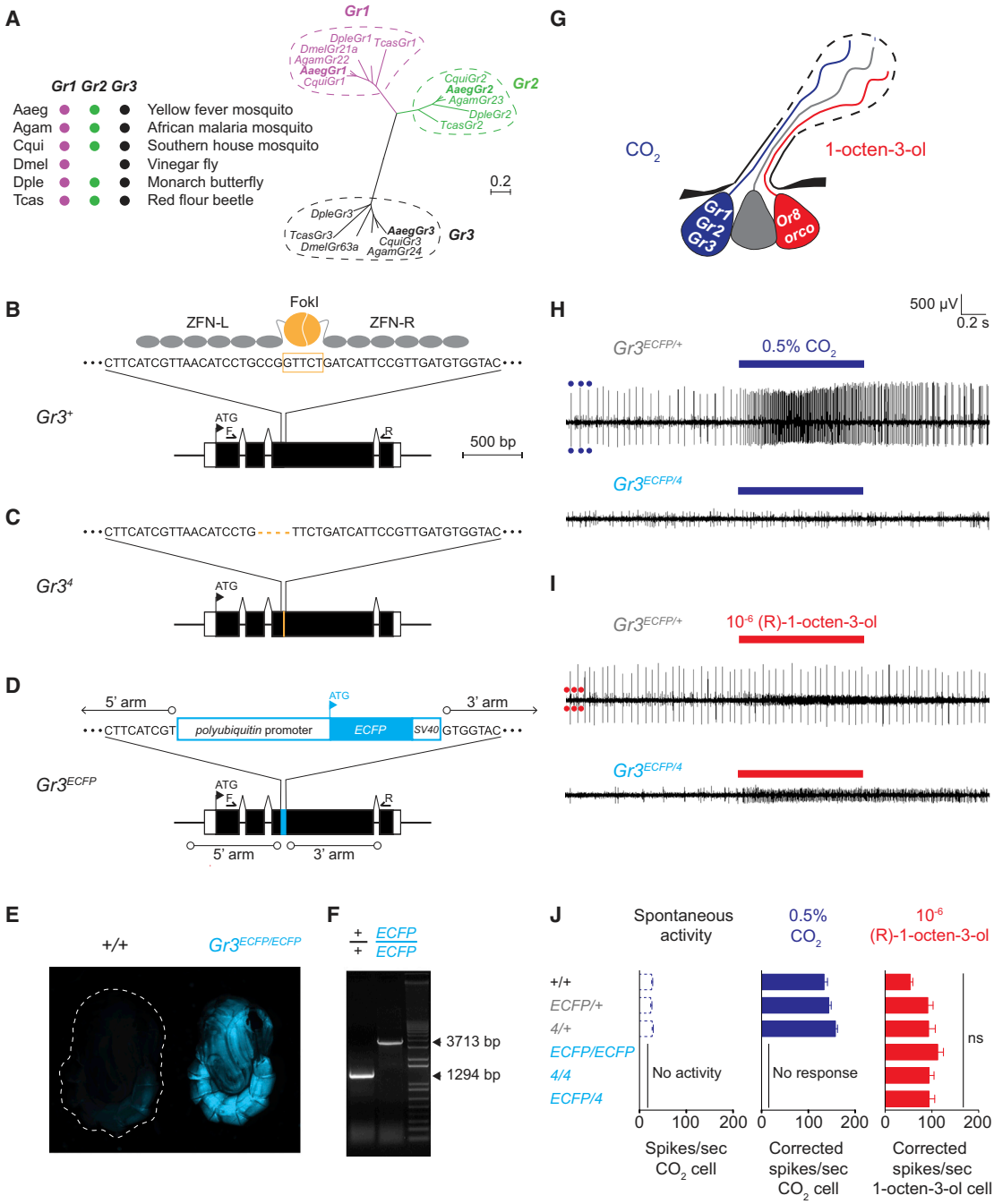


**Figure 1. Electrophysiological Characterization of *Gr3* Mutants Generated by ZFN Gene Editing**

(A) Phylogenetic comparison of insect $CO_2$ receptor genes. Aaeg: *Aedes aegypti*, Agam: *Anopheles gambiae*, Cqui: *Culex quinquefasciatus*, Dmel: *Drosophila melanogaster*, Dple: *Danaus plexippus*, Tcas: *Tribolium castaneum*. Branch lengths are proportional to sequence divergence. Scale bar, 0.2 amino acid replacements per site.

(B) The *Ae. aegypti Gr3* genomic locus, with a schematic of the *Gr3* ZFN pair binding to exon 3 DNA and the Fok1 cleavage site indicated in orange.

(C) Diagram of 4 bp deletion in the mutant $Gr3^{4}$ genomic locus.

(D) Diagram of the mutant $Gr3^{ECFP}$ genomic locus.

(E) Representative fluorescent images of female wild-type and $Gr3^{ECFP/ECFP}$ mutant pupae.

(F) PCR products generated across the *ECFP* insertion site using the F and R primers indicated by small arrows in (B) and (D).

(G) Diagram of receptor expression and ligand specificity of maxillary palp capitate peg sensillum OSNs.

(H) Representative spike traces during extracellular recordings from a $Gr3^{ECFP/+}$ heterozygous (top) and $Gr3^{ECFP/4}$ mutant (bottom) capitate peg sensillum evoked by 0.5% $CO_2$. Dark blue circles mark large amplitude spikes from the $CO_2$-sensitive OSN. Stimulus bar (blue): 1 s.

*(legend continued on next page)*

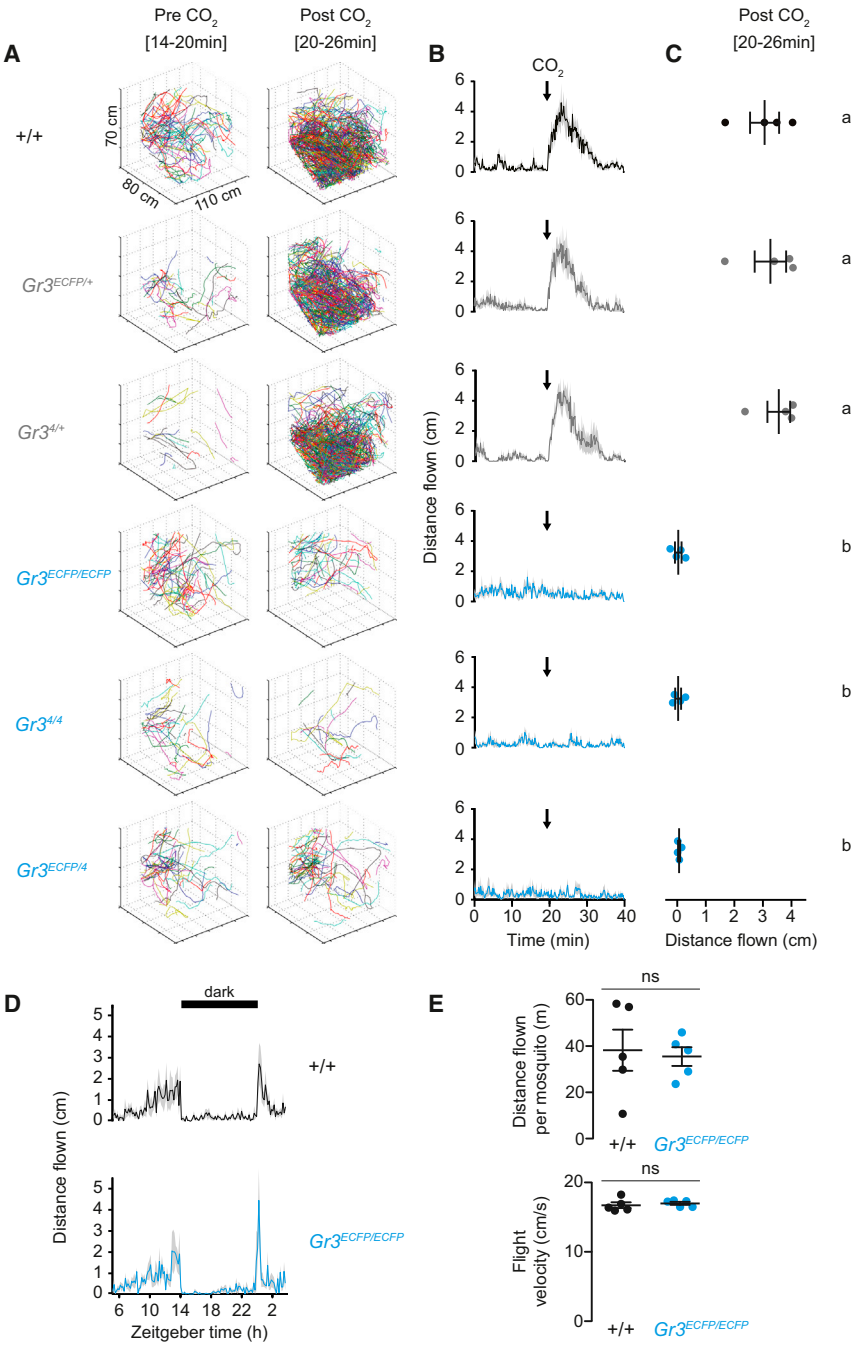


**Figure 2. *Ae. aegypti Gr3* Mutants Are Not Activated by $CO_2$ and Retain Normal Locomotor Behavior**

(A–C) $CO_2$-evoked flight activity of groups of female *Ae. aegypti* wild-type, heterozygous, and mutant mosquitoes tracked for 20 min before and after a 40 s pulse of $CO_2$ (n = 4 replicates per genotype; n = 20 mosquitoes/trial).

(A) Representative 3D tracks of the indicated genotypes in the 6 min pre- (left) and post-application (right) of a 40 s pulse of $CO_2$.

(B) Distance flown (cm/s/animal) in response to stimulation with $CO_2$ (black arrow). Data are shown as mean (solid line) ± SEM (gray shading).

(C) Mean distance flown per second for mosquitoes post-application of $CO_2$ (t = 20–26min). Each replicate is indicated by a dot, and mean ± SEM as bars. Variation among genotypes was significant (one-way ANOVA, $p < 0.0001$). Genotypes marked with different letters are significantly different by post hoc Tukey's HSD test ($p < 0.001$).

(D) Locomotor activity of wild-type and $Gr3^{ECFP/ECFP}$ mutant mosquitoes measured as cm/min/animal over a 23 hr period (dark period indicated by black bar) without supplemental $CO_2$ (n = 5 replicates per genotype; 20 females per replicate). Data are shown as mean (solid line) ± SEM (gray shading).

(E) Total distance flown per mosquito and average flight velocity of data in (D). Each replicate is indicated by a dot, and mean ± SEM as bars (ns, not significant; t test, $p > 0.05$).

increase in capture rate in both ports may reflect random exploratory behavior of females in the two-port assay chamber upon activation with $CO_2$ in the absence of other olfactory cues. This contrasts with the known attraction of mosquitoes to $CO_2$ in a wind tunnel (Dekker and Cardé, 2011), likely because $CO_2$ is not presented as a filament in our two-port assay. Responses to $CO_2$ alone were abolished in $Gr3^{ECFP/ECFP}$ mutants, consistent with their inability to sense this stimulus (Figure 4C).

We next evaluated responses to L-(+)-lactic acid, a volatile organic compound present in human breath and skin odor, which has previously been shown to synergize behaviorally with $CO_2$ to enhance mosquito attraction (Acree et al., 1968; Eiras and Jepson, 1991). L-(+)-lactic acid was not attractive to female mosquitoes when presented alone (Figure 4D). However, when L-(+)-lactic acid was presented with $CO_2$, many wild-type and heterozygous females were attracted. $Gr3^{ECFP/ECFP}$ mutants did not respond in these same trials, indicating that $CO_2$ detection is required for synergistic responses to lactic acid (Figure 4E).

(I) Representative spike traces from heterozygous and mutant basiconic sensilla evoked by $10^{-6}$ (R)-1-octen-3-ol. Red circles mark small amplitude spikes from the 1-octen-3-ol-sensitive OSN. Stimulus bar (red): 1 s.

(J) Summary of spontaneous activity and $CO_2$- and (R)-1-octen-3-ol-evoked responses in the indicated genotypes. Data are presented as mean ± SEM. Genotypes did not differ in their response to (R)-1-octen-3-ol (one-way ANOVA, $p = 0.07$; ns, not significant; n = 8–16 sensilla recorded from at least three mosquitoes per genotype).

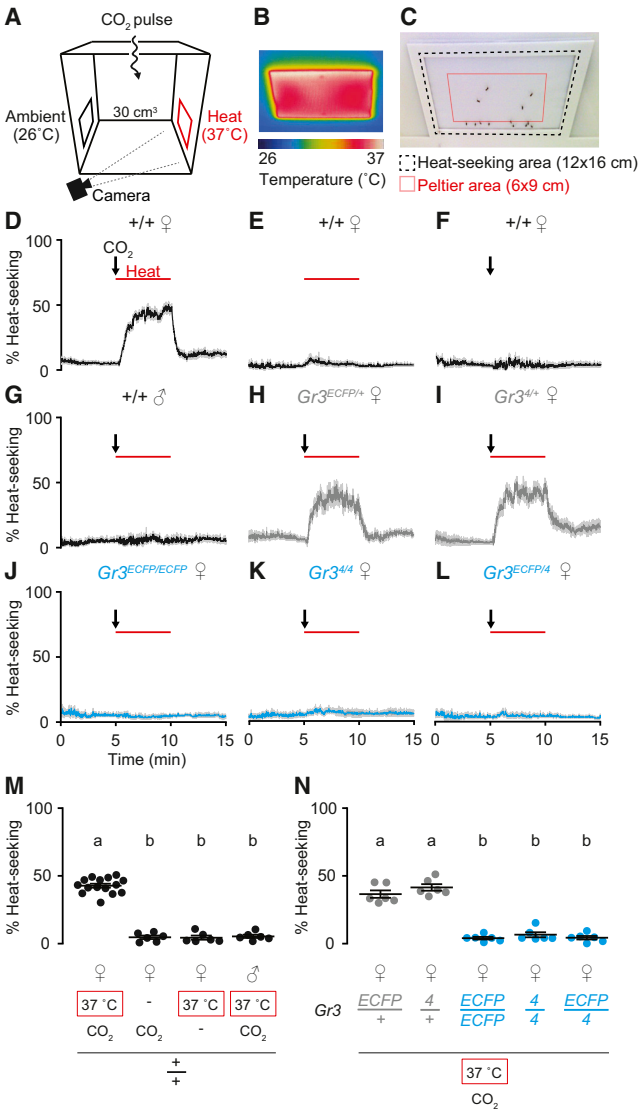


**Figure 3. $CO_2$ Detection Gates Heat-Seeking Behavior in Female *Ae. aegypti***

(A) Schematic of the mosquito heat-seeking assay.

(B) Thermal image of target Peltier heated to 37°C.

(C) Image indicating Peltier location (red outline) and area scored for heat seeking (black dashed line).

(D–L) Mosquitoes of the indicated sex and genotype seeking an ambient or heated target, with or without a pulse of $CO_2$. The 5 min 37°C stimulus is indicated by the red bar. The 20 s pulse of $CO_2$ is indicated by the black arrow. Data are shown as mean (solid line) ± SEM (gray shading) (n = 6 trials, except D, where n = 15; 20–25 mosquitoes/trial).

(M and N) Quantification of heat seeking during minutes 7–10 of assay. Each replicate is indicated by a dot, and mean ± SEM as bars. Variation among both stimulus regimes and mosquito genotypes was significant (one-way ANOVA, $p < 0.0001$ for both M and N). Data labeled with different letters are significantly different using Tukey's HSD test comparing all pairs of means ($p < 0.001$).

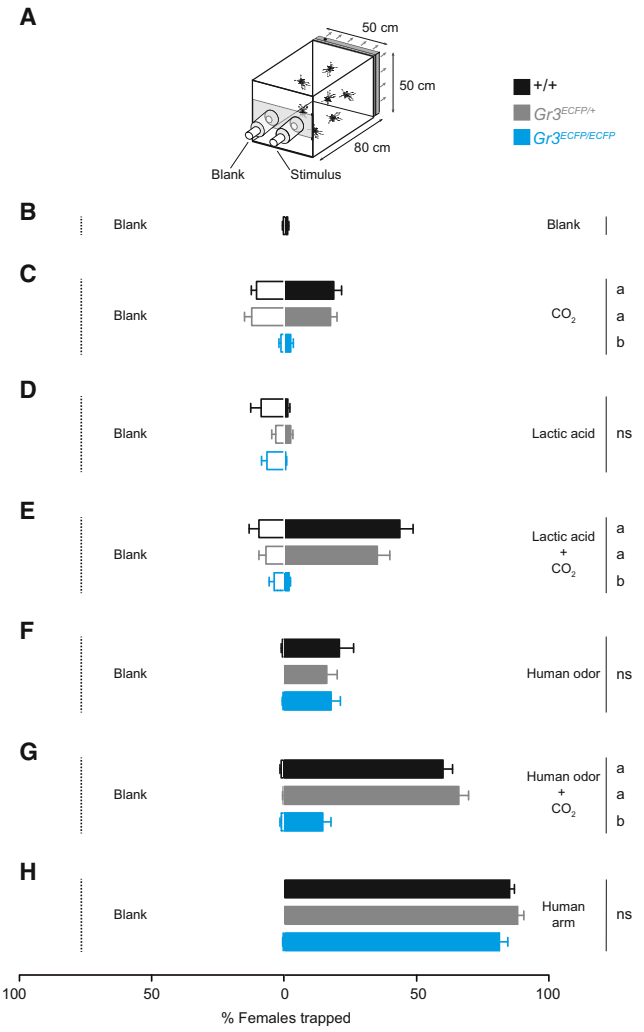


**Figure 4. $CO_2$ Synergizes with Host Odor to Drive Mosquito Attraction**

(A) Diagram of the two-port olfactometer.

(B–H) Response of the indicated genotypes to a choice of the blank port compared to the stimulus indicated at the right. Data are plotted as mean ± SEM (n = 8–11 trials per condition; n = 50 mosquitoes per trial). Significance was assessed with one-way ANOVA. Genotypes marked with different letters are significantly different by Tukey's HSD test ($p < 0.0001$; ns, not significant).

To evaluate whether $CO_2$ detection modulates perception of human skin odor, we examined mosquito responses to human odor collected on nylon sleeves. Human odor in the absence of $CO_2$ elicited moderate attraction that was not significantly different among genotypes (Figure 4F). However, supplementation of $CO_2$ to human odor enhanced levels of attraction observed for wild-type and heterozygous females, but not homozygous mutants (Figure 4G).

To assess a more complex multisensory stimulus, we tested mosquito attraction to a live human arm inserted into the stimulus port. Very high levels of attraction were observed for all mosquito genotypes to a live human arm in this assay (Figure 4H). We speculate that additional stimuli presented by the human arm, including odorants not trapped on nylon sleeves, moisture, heat, and visual cues, overcome the behavioral defect seen with simpler stimulus combinations in the mutants.

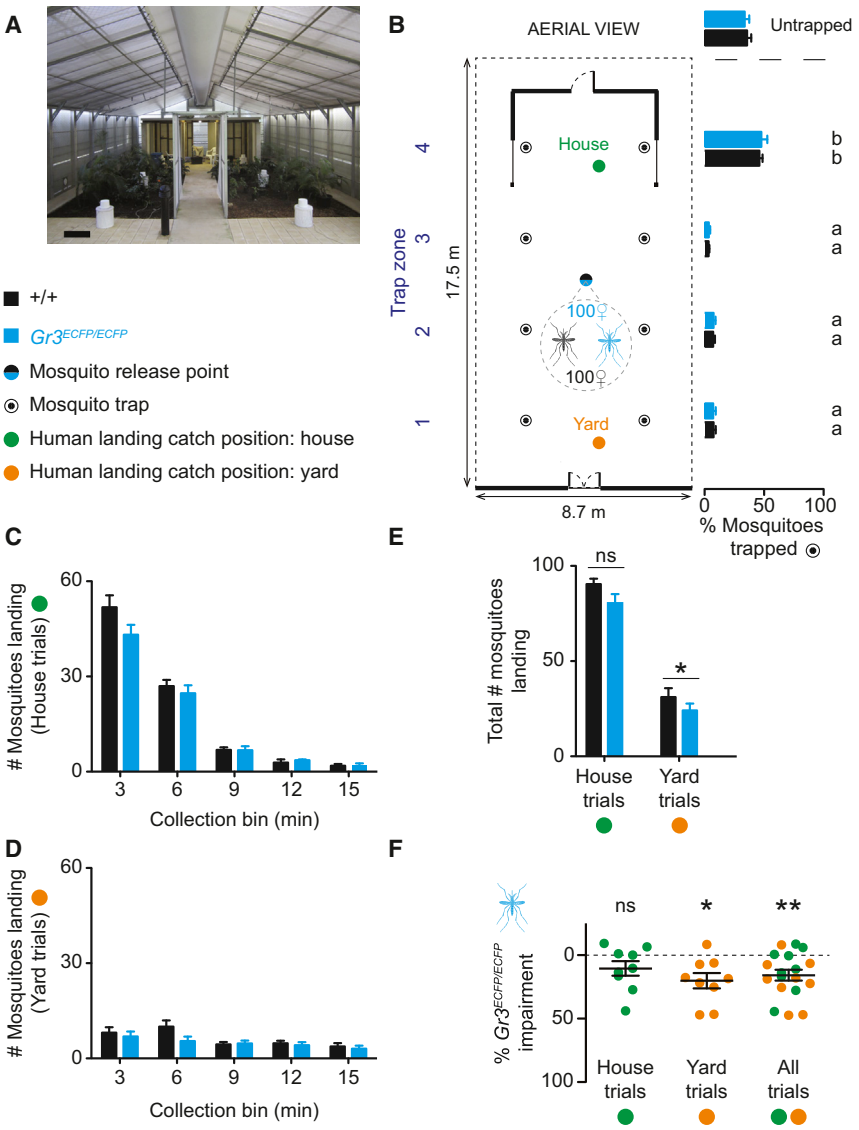


**Figure 5. *Gr3* Mutants Have Diminished Responses to Live Humans in a Semi-Field Environment**

(A) Interior view of the semi-field cage. Scale bar, 0.5 m.

(B) Schematic of the semi-field cage showing the average distribution of an equal mix of wild-type and $Gr3^{ECFP/ECFP}$ mutant female mosquitoes (n = 100 per genotype) in the cage in the absence of humans (n = 5 trials). Distribution varied significantly according to trap zone but not genotype (two-way ANOVA, $p < 0.0001$ for trap zone and $p = 0.773$ for genotype). Different letters indicate significantly different means by post hoc Tukey's HSD test.

(C and D) Number of mosquitoes of the indicated genotype landing on human subjects in 3 min bins during 15 min at house (C) or yard (D) position (n = 9 trials per position).

(E) Total number of mosquitoes landing in human-landing catch trials with human volunteers at house or yard position. Paired t tests were used to assess statistical significance in comparisons between genotypes (ns, not significant; $p = 0.09$; *$p = 0.018$).

(F) Relative impairment in host-seeking of $Gr3^{ECFP/ECFP}$ mutants compared to wild-type mosquitoes (one-sample t test relative to zero; ns, not significant; $p = 0.105$; *$p = 0.011$; **$p = 0.002$).

In (B)–(F), all data are plotted as mean ± SEM.

## Mosquito Attraction to Humans in a Semi-Field Environment Is Diminished but Not Abolished in *Gr3* Mutants

To obtain a more biologically relevant estimate of the contribution that $CO_2$ detection makes to mosquito host attraction, we tested the ability of *Gr3* mutants and wild-type females to locate and land on live human volunteers in the James Cook University semi-field cage in Northern Queensland, Australia (Figure 5A). This semi-field cage contained the underside of an elevated Queenslander style house, including furniture used as resting sites of *Ae. aegypti*, and a lush tropical backyard that mimicked the native habitat of *Ae. aegypti* in this region (Ritchie et al., 2011). Equal numbers of wild-type and mutant females were released into the semi-field cage during each trial for simultaneous comparisons of mosquito host-seeking behavior.

To examine the distribution of the released mosquito population over the semi-field cage without humans present, we used mosquito traps to capture females in four designated trap zones (Figure 5B, left). The majority of the mosquitoes of both genotypes were trapped near the house, and there were no differences between the numbers of each mosquito genotype trapped in each zone (Figure 5B, right). Therefore, under semi-field conditions, both wild-type and *Gr3* mutant mosquitoes retained an innate preference for human habitation. The mutants showed similar dispersal across the semi-field cage relative to wild-type mosquitoes, consistent with their performance in flight-tracking assays (Figures 2D and 2E).

To test mosquito attraction to humans, we counted the number of wild-type and mutant mosquitoes landing on a seated volunteer positioned within either the house or yard of the semi-field cage (Figure 5B, green and orange circles, respectively). The mosquito traps were inaccessible during human-landing catch trials. Slightly fewer *Gr3* mutants landed on humans compared to wild-type mosquitoes during the initial two collection bins of house and yard trials (Figures 5C and 5D). These small cumulative differences were maintained over the duration of each assay, leading to fewer *Gr3* mutants being collected in total on average compared to wild-type mosquitoes at either human-landing catch position (Figure 5E). Overall, landing varied significantly according to genotype ($p = 0.043$) and position in the cage ($p < 0.0001$), but a two way-ANOVA showed that there was no interaction between these two variables ($p = 0.713$). Variation in mosquito landings between

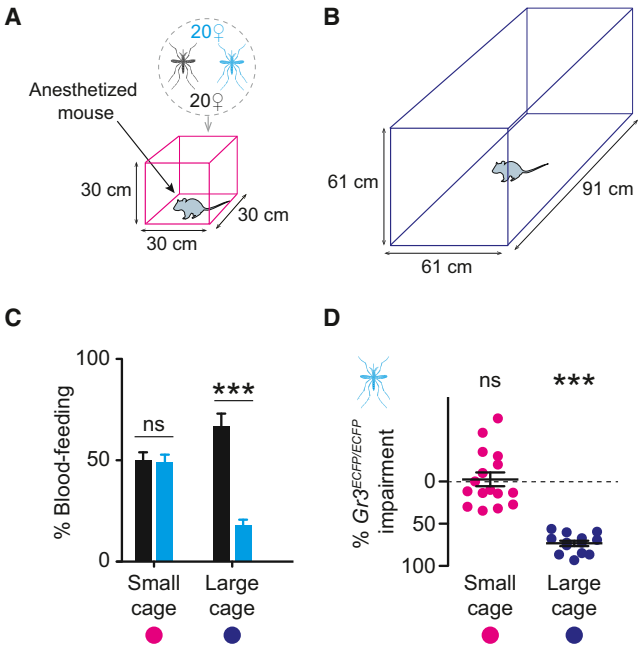


**Figure 6. Spatial Scale-Dependent Responses of *Gr3* Mutants to Live Animal Hosts**

(A and B) Diagrams of small (A) and large (B) cage assays. Mice not to scale.

(C and D) Percent blood feeding of the indicated genotype (C) and impairment of $Gr3^{ECFP/ECFP}$ mutants relative to wild-type (D).

Significance was assessed in (C) with paired t tests and in (D) with a one-sample t test relative to zero (ns, not significant; ***$p < 0.0001$).

All data are plotted as mean ± SEM (small cage: n = 16 trials; large cage: n = 13 trials; n = 20 mosquitoes/genotype/trial).

human volunteers was not significant (data not shown). Overall, $Gr3^{ECFP/ECFP}$ mosquitoes were impaired by approximately 15% relative to wild-type mosquitoes in the semi-field cage (Figure 5F). Thus, a loss of $CO_2$ detection diminishes but does not abolish the ability of mosquitoes to find humans in the semi-field cage.

## Effects of $CO_2$ Sensation on Mosquito Host-Seeking Behavior Are Dependent on Spatial Scale

Host sensory cues such as heat, $CO_2$, human odor, moisture, and visual contrast are most potent when a mosquito is close to the human host and decline at a distance. We therefore reasoned that the host-seeking defects in *Gr3* mutants would depend on spatial scale, such that a more dramatic defect would be apparent if the mutants were tested in a larger semi-field cage. Because to our knowledge no larger semi-field facilities currently exist, we modeled host-seeking behavior at two different spatial scales with live animal hosts in laboratory cages of different sizes (Figures 6A and 6B).

In these assays, mixed populations of equal numbers of wild-type and $Gr3^{ECFP/ECFP}$ mosquitoes were released into each cage and assayed for their ability to blood-feed on an anesthetized mouse. Similar numbers of wild-type and $Gr3^{ECFP/ECFP}$ females blood-fed during trials in the small (0.027 $m^3$) cage, but significantly fewer *Gr3* mutant females blood-fed relative to wild-type mosquitoes in the larger (0.339 $m^3$) cage (Figure 6C). On average, blood-feeding rates in $Gr3^{ECFP/ECFP}$ females were unimpaired in the small cage consistent with semi-field cage results but impaired by approximately 70% relative to wild-type mosquitoes in the larger cage (Figure 6D). Two-way ANOVA on blood-feeding rates revealed a highly significant interaction ($p < 0.0001$) between mosquito genotype and cage size, suggesting that the effects of $CO_2$ sensation on host-seeking behavior are dependent on spatial scale. We note that presence of wild-type mosquitoes did not rescue the major deficits in host seeking seen in $Gr3^{ECFP/ECFP}$ mutants in the large cage (Figure 6C). This rules out the possibility that motor, auditory, or pheromonal cues from wild-type mosquitoes influence the behavior of mutant mosquitoes in this assay.

## Sensory Stimuli Synergize in Multiple Binary Combinations to Drive Mosquito Blood-Feeding Behavior

Given that $CO_2$ is a major host-seeking cue and strongly influences mosquito perception of heat and odorants, we were intrigued by the nearly normal attraction of homozygous *Gr3* mutants to live humans in a semi-field environment. To ask how the phenotypic deficits of *Gr3* mutants may be compensated during attraction to live hosts, we developed an artificial membrane-feeding assay (Figure 7A) to test the contribution of individual and combined sensory cues including $CO_2$, heat, and human odor to mosquito blood-feeding behavior.

To test whether heat and $CO_2$ are integrated to drive blood-feeding behavior, we manipulated the temperature of blood inside the membrane feeder to reflect human body (37°C) or ambient (26°C) temperatures in the presence or absence of $CO_2$. Wild-type and heterozygous mosquitoes blood-fed from membrane feeders only when the blood was heated to 37°C and $CO_2$ was added to the assay (Figure 7B). Homozygous *Gr3* mutants rarely blood-fed under these conditions (Figure 7C).

We then tested whether human odor presented with heat can rescue blood feeding in *Gr3* mutants. Very few females of any genotype blood-fed from a heated membrane feeder in the absence of other cues (Figure 7D). Human odor when applied alone to a membrane feeder filled with ambient-temperature blood also elicited low levels of blood feeding (Figure 7E). However, when we applied human odor to the membrane of heated feeders, we observed high rates of blood feeding in all genotypes (Figure 7F).

To determine whether $CO_2$ and odor cues can also synergize to drive blood feeding in the absence of heat, we applied human odor to a membrane feeder maintained at ambient conditions and added $CO_2$. High numbers of wild-type and heterozygous mosquitoes, but very few homozygous *Gr3* mutants, blood-fed on this room-temperature blood (Figure 7G). Taken together, these results indicate that $CO_2$, odor, and heat synergize in all possible binary combinations to drive *Ae. aegypti* blood-feeding behavior.

## DISCUSSION

Here we used ZFN-mediated targeted mutagenesis and homologous recombination to target the *Ae. aegypti Gr3* gene to

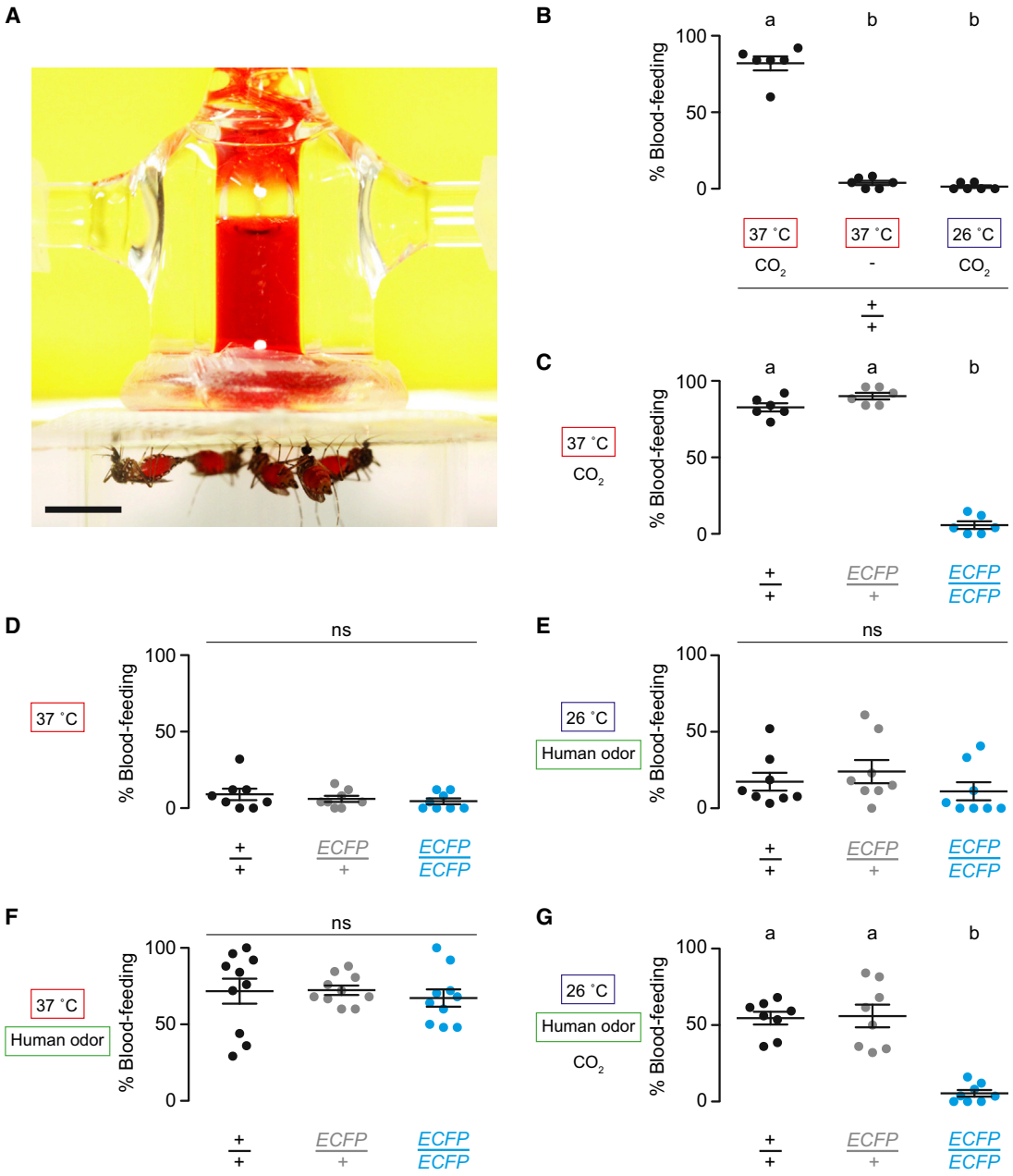


**Figure 7. Multiple Host Sensory Cues Combine to Elicit Mosquito Blood-Feeding Behavior**

(A) Image of female *Ae. aegypti* mosquitoes blood feeding from a glass membrane feeder. Scale bar, 0.5 cm.

(B) Blood-feeding responses of wild-type mosquitoes with different blood temperatures and ± $CO_2$.

(C–G) Blood-feeding responses of the indicated genotypes with different blood temperatures ± $CO_2$ ± human odor.

In (B)–(G), significance was assessed with one-way ANOVA. Data labeled with different letters are significantly different using Tukey's HSD test ($p < 0.001$; ns, not significant). Replicate data points and mean ± SEM are shown (n = 6–10 trials/genotype and condition; n = 25 mosquitoes per trial).

generate mosquitoes unable to detect or behaviorally respond to volatile $CO_2$. Interestingly, mutating only *Gr3* while sparing *Gr1* and *Gr2* was sufficient to disrupt $CO_2$ responses. This suggests that this subunit plays an essential role not compensated for by the two remaining $CO_2$ receptor subunits. The stoichiometry of the $CO_2$ receptors in *Aedes, Anopheles*, and *Drosophila* currently remains unknown. In *Drosophila*, it has been shown that the two $CO_2$ receptor subunits together reconstitute a functional receptor (Jones et al., 2007; Kwon et al., 2007). Ectopic expression of *An. gambiae* $CO_2$ receptor subunits in *Drosophila* OSNs suggests that *Gr1* and *Gr3*, as well as the combination of *Gr1*, *Gr2*, and *Gr3*, form a functional $CO_2$ receptor (Lu et al., 2007). In *Ae. aegypti*, transient RNAi knockdown experiments that assessed mosquito orientation toward a $CO_2$ source suggested

that *Gr1* and *Gr3* but not *Gr2* play a role in $CO_2$ reception (Erdelyan et al., 2012). The respective functional contribution of *Gr1* and *Gr2* to $CO_2$ detection therefore remains unclear and awaits further genetic and biochemical characterization. It will be interesting to determine whether all three subunits are functionally required to detect $CO_2$ or whether *Gr1* and *Gr2* are functionally redundant. Further, it is not known whether one $CO_2$ receptor subunit functions as a non-ligand-selective coreceptor whereas others interact with the ligand, as is the case with insect odorant receptors and ionotropic receptors (Benton et al., 2009; Larsson et al., 2004).

Several volatile odorants have recently been shown to antagonize, activate, or hyperactivate the $CO_2$ neuron in a variety of mosquito species, in some instances leading to behavioral disorientation (Lu et al., 2007; Tauxe et al., 2013; Turner et al., 2011). The availability of *Gr3* mutants will allow us to ask whether these compounds act through the $CO_2$ receptor complex or through other uncharacterized receptors or signaling machinery associated with this neuron. Further, multiple odorants have been shown to antagonize responses from the $CO_2$ neuron and to reduce mosquito attraction when applied at high concentration ($10^{-1}$) to human skin (Tauxe et al., 2013). We suggest that these chemicals are unlikely to mask attraction to humans via a loss of activity in the $CO_2$ receptor complex alone because $CO_2$-insensitive *Gr3* mutants remain highly attracted to live humans in our semi-field assays. Whether these odorants also activate additional mosquito chemosensory receptors on the antenna, palp, or proboscis at high concentration to elicit mosquito repulsion remains to be determined.

Our behavioral data support the conclusion that multimodal integration of $CO_2$, heat, and odor drives host-seeking and blood-feeding behavior in *Ae. aegypti*. We show that $CO_2$ gates mosquito perception of both heat and the monomolecular attractant lactic acid. This binary synergism extended to other combinations of sensory stimuli, including human skin odor with heat or $CO_2$. This synergism of multiple sensory cues may explain why attraction to live humans was diminished but not abolished in *Gr3* mutants in semi-field and two-port olfactometer trials. Interestingly, we also observed that synergy between $CO_2$ and host odor was sufficient to induce wild-type female mosquitoes to blood-feed on unheated blood. Consistent with this notion, *Ae. aegypti* have been observed to blood-feed on cold-blooded animals such as lizards when warm-blooded vertebrates were unavailable (Woke, 1937).

The absence of a major deficit in *Gr3* mutant attraction to live humans in the semi-field cage tested here does not preclude the possibility that more pronounced effects may have been observed if the human host was presented in a larger semi-field cage. Indeed, we used tests with animal hosts presented in small or large cages to determine that the effects of $CO_2$ detection on host-seeking behavior appear to be dependent on spatial scale. Synergism between multiple remaining sensory cues including visual contrast, moisture, heat, and volatile odorants from the skin and breath may explain why attraction to live humans was diminished but not abolished in *Gr3* mutants in our assays.

When combined, heat and human odors have been found to influence cross-wind flight behavior and increase source-finding and landing responses in female *An. gambiae* (Spitzen et al., 2013). Although it is not known over what distance mosquitoes perceive heat, it is generally assumed that thermal convection currents emanating from human skin rapidly dissipate to reach equilibrium with ambient temperature conditions within $\leq$1.5 m of the host (Lewis et al., 1969; Spitzen et al., 2013). Synergistic interactions between human odor or $CO_2$ with heat may potentially act over short distances to guide landing behavior as mosquitoes approach hosts.

Previous studies suggested that *Ae. aegypti* is attracted to both stationary and moving visual contrast, and that the activating effects of human scent combined with visual feedback allow mosquitoes to navigate upwind toward hosts (Kennedy, 1940). In addition, it is possible that diurnal patterns of flight periodicity in *Ae. aegypti* (Trpis et al., 1973) may randomly bring females into the effective range of host cues where multimodal integration may then occur. The role of mosquito vision in host-seeking and its interactions with odors warrants further investigation.

Multisensory integration allows organisms to form salient percepts from combined sensory stimuli to drive context-dependent behaviors. An example of such integration in humans is the fusion of smell and taste of food or drink into the single percept of flavor (reviewed in Small, 2012). Neither chemosensory input in isolation fully encodes the experience of the food or beverage, which may explain why humans with olfactory dysfunction report difficulties with enjoyment of food and wine (Keller and Malaspina, 2013). Another benefit of multisensory integration is improvement in the reliability of signal detection. In noisy auditory environments, verbal comprehension can be improved dramatically by the practice of lip reading, thus combining auditory and visual perception to enhance the accuracy of signal detection (reviewed in Campbell, 2008). For the female mosquito, such multisensory integration may be crucial for efficient host seeking in a cluttered sensory environment. In the case of female mosquitoes living near human settlements, there are likely to be many sensory distractors in the environment that emit heat, human scent, or $CO_2$ in isolation. By requiring the simultaneous presentation of at least two such cues before host-seeking behavior is triggered, the mosquito increases her chances of high-fidelity host localization. Furthermore, body odor is itself a complex blend of multiple odorants that acts to shape both mosquito host preference (DeGennaro et al., 2013) and the tendency of *Ae. aegypti* and *An. gambiae* to bite certain regions of the body including the lower legs, ankles, and feet (reviewed in Smallegange et al., 2011).

What are the neural mechanisms employed by the female mosquito to integrate sensory cues to trigger attraction to humans? One can envision peripheral mechanisms by which $CO_2$ or heat directly sensitize peripheral odor-detecting OSNs, but no such mechanism has yet been described in insects. Conversely, odors have been shown to affect responses of the $CO_2$ OSN (Lu et al., 2007; Tauxe et al., 2013; Turner et al., 2011), but this modulation required very high odor concentrations unlikely to be attained in human skin odor. A more plausible mechanism would be central integration of these cues, as is known to occur for human taste and smell integration in the anterior ventral insula (reviewed in Small, 2012). One can imagine odor and $CO_2$ synergy occurring early in sensory

processing pathways because both send afferents to the antennal lobe (Anton et al., 2003). Much less is known about what brain areas process heat cues, so it seems plausible that higher brain centers are responsible for the synergistic interactions reported here. It is intriguing that male mosquitoes do not show synergy between $CO_2$ and heat sensation. We presume that this is not due to defects in primary detection of the cues but more likely due to differences in wiring the male brain or its susceptibility to modulation by multiple sensory inputs. The availability of genetically encoded calcium sensors and novel circuit-tracing methods (Ruta et al., 2010) opens up the possibility of carrying out functional imaging in the mosquito brain to reveal the anatomical sites and mechanisms of multisensory integration.

The ability of *Ae. aegypti* to improve host source localization via multimodal integration of sensory cues could act to increase the probability that the female mosquito obtains a blood meal, a behavior inextricably linked to mosquito reproduction. Because integration between any pairing of $CO_2$, heat, and host odor is sufficient to drive mosquito blood feeding, chemicals targeting a single sensory modality (Tauxe et al., 2013; Turner et al., 2011; Jones et al., 2011) may be less effective in perturbing mosquito behavior than their combined use to disrupt multiple sensory pathways. Such synergistic approaches to manipulate mosquito sensory perception may ultimately yield a powerful strategy to deter mosquitoes from finding humans.

## EXPERIMENTAL PROCEDURES

### Mosquito Rearing and Maintenance

*Ae. aegypti* wild-type (*Orlando*) and *Gr3* mutant strains were maintained and reared at 25°C–28°C, 70%–80% relative humidity, with a photoperiod of 14 hr light:10 hr dark (lights on 8 a.m.) as previously described (DeGennaro et al., 2013). Adult mosquitoes were provided constant access to 10% sucrose solution for feeding. Females were provided with a blood source for egg production. All laboratory blood-feeding procedures with mice and humans and use of humans in behavioral assays were approved and monitored by The Rockefeller University Institutional Animal Care and Use Committee and Institutional Review Board, protocols 11487 and LVO-0652, respectively. Semi-field cage experiments performed with human subjects at James Cook University were approved and monitored by the JCU Institutional Biosafety Committee and Human Research Ethics Committee (Ethics approval H4450). All human subjects gave their informed consent to participate in laboratory and semi-field experiments. Female mosquitoes used for electrophysiological and behavioral assays were 5–10 days old and mated but not blood-fed. Before behavioral assays, mosquitoes were sexed and sorted under hypothermia (4°C) or aspiration and fasted for 14–24 hr in the presence of a water source.

### Phylogenetic Analysis

Amino acid alignment and phylogenetic analysis of insect $CO_2$ receptor genes were performed with MegAlign version 8.0.2 (DNASTAR) using the ClustalW and neighbor-joining methods. The phylogenetic tree was visualized as a radial phylogram using Dendroscope version 3.2.8 (Huson and Scornavacca, 2012).

### ZFN-Targeted Mutagenesis and Homologous Recombination

ZFNs targeting *Ae. aegypti Gr3* were produced by the CompoZr Custom ZFN Service (Sigma-Aldrich Life Science). Details of the design of the ZFNs and isolation of deletion and homologous recombination mutants are in the Extended Experimental Procedures.

### Single Sensillum Electrophysiology

Extracellular recordings of $CO_2$ (Matheson Tri-Gas) and (R)-1-octen-3-ol (C.A.S. 3687-48-7, Bedoukian) responses from female maxillary palp capitate peg sensilla of the indicated genotype were carried out as previously described (DeGennaro et al., 2013; Pellegrino et al., 2010). All capitate peg sensilla sampled from wild-type and *Gr3* heterozygous mosquitoes responded to both (R)-1-octen-3-ol and $CO_2$. Corrected spike increases were calculated by subtracting the spontaneous activity for 1 s before stimulus application from the activity evoked during 1 s of stimulus. Spontaneous activity was determined by counting spikes for 1 s prior to the application of paraffin oil (Sigma-Aldrich) to the same sensillum.

### Three-Dimensional Multi-Insect Tracking System

A multi-insect 3D tracking system was custom designed and built in collaboration with SciTrackS GmbH. Details of the fabrication and operation of the system are in the Extended Experimental Procedures.

### Heat-Seeking Assay

For each 15 min trial, 20–25 mosquitoes were introduced into a custom-made Plexiglass box (30 × 30 × 30 cm) and allowed to acclimate for 5 min. Two Peltier elements (6 × 9 cm surface area; Tellurex) located on opposite walls of the enclosure, and covered with white paper and white plastic mesh, were used to present heat stimuli. During acclimation, both Peltiers were kept at ambient temperature (26°C) via controllers (Oven Industries) commanded by a custom MATLAB script. Throughout the trial, carbon-filtered air was pumped into the box via a diffusion pad (59-144, Flystuff.com) installed on the ceiling of the enclosure. After acclimation, 10% $CO_2$ was added to the air stream for 20 s via a solenoid valve (Parker-Hannifin) to increase $CO_2$ concentration 1,000 ppm above background levels. At this time, one Peltier was warmed to 37°C for 5 min and subsequently cooled to ambient for the remaining 5 min of the trial. The side of the heated Peltier was randomized across trials. Mosquito landings at the Peltier were monitored by fixed cameras (FFMV-03M2M-CS, Point Grey Research) acquiring images at 1 Hz. We noted that mosquitoes were attracted to the Peltier surface as well as to adjacent surfaces, presumably due to heat dissipation and convective currents. Therefore, images were analyzed using custom MATLAB scripts to count heat-seeking mosquitoes within a fixed target region comprising a 12 cm × 16 cm area around the center of the Peltier. Peltier surface temperatures were measured using a thermal imaging camera (E60, FLIR).

### Two-Port Olfactometer Assays

Two-port olfactometer assays were performed as previously described (DeGennaro et al., 2013). Experimental details are in the Extended Experimental Procedures.

### Semi-Field Cage and Human-Landing Catch Assays

Semi-field cage experiments were conducted at the James Cook University Mosquito Research Facility Semi-Field System (Ritchie et al., 2011) in Cairns, Queensland, Australia from January 11, 2013–February 5, 2013. Mated, nulliparous 5- to 10-day females were used for these assays. Prior to use, mosquitoes were sexed via aspiration and fasted for 16 hr in holding containers with access to water only. To populate the semi-field cage for human-landing catch trials, at 10 a.m. each day, an equal mix of 100 each wild-type *Orlando* and $Gr3^{ECFP/ECFP}$ mutant female mosquitoes was released from a central release point in the cage (Figures 5A and 5B). Mosquitoes were allowed to disperse across the cage and acclimate to semi-field conditions for 5 hr. At 3 p.m. each day, a human volunteer entered the cage and sat down for a period of 15 min at one of two predesignated human-landing catch positions: either within the house structure or 11 m away in the yard of the cage (Figure 5B). During each trial, volunteers wore full-length white lab coats to standardize visual cues and used a hand-held mechanical aspirator (model 2809C, BioQuip Products) to collect mosquitoes that landed on their exposed legs and ankles. Mosquitoes were aspirated during five consecutive 3 min collection windows across each 15 min trial period using separate aspirator cartridges (2809V, BioQuip Products). The number of wild-type and $Gr3^{ECFP/ECFP}$ mutant mosquitoes landing on each volunteer was then scored post hoc by assaying tissue homogenates from each collected mosquito for *ECFP* fluorescence using a

POLARstar Omega microplate reader (BMG Labtech) equipped with a 440/485 nm excitation-emission filter set. To prepare samples for analysis, whole mosquitoes were homogenized at 4°C in 2 ml microcentrifuge tubes containing 100 μl PBS (pH 7.2) (GIBCO) with 2 mm borosilicate beads (Sigma-Aldrich) using a QIAGEN TissueLyser II (QIAGEN) set to maximum speed for 5 min. Samples were centrifuged at 12,100 × g at 4°C for 5 min to pellet debris and obtain a soluble protein fraction that was assayed in triplicate for *ECFP* fluorescence on black 384-well small volume HiBase polystyrene microplates (784076, Greiner Bio-One). Three adult male volunteers (ages 27–46) participated in human-landing catch trials. Each volunteer was tested three times in each of the two house and yard positions (n = 9 trials total per position). A single experimental replicate was performed each day.

In separate experiments, the distribution of wild-type and $Gr3^{ECFP/ECFP}$ mosquitoes in the cage in the absence of humans was determined using eight Biogents Sentinel (BGS) Mosquito traps (Biogents GmbH) devoid of chemical lures and symmetrically placed, two in each of four trap zones, across the semi-field cage (Figures 5A and 5B). During BGS trials (n = 5), each mixed population of 100 females per strain was released at 9 a.m., and mosquitoes were allowed to distribute across the cage for 1 hr. After this acclimation period, traps were uncovered and turned on until 5 p.m. the same day. The BGS trap socks containing catches were then collected and emptied, and mosquitoes genotyped as described above.

Between experimental replicates, the semi-field cage was further depleted of all remaining mosquitoes by a mass-trapping procedure using 1 hr human-landing catches, mechanical aspiration, and continuous BGS trap runs. Cage depletion between replicates was verified in the morning prior to initiating the next experimental replicate by the prerequisite condition that no mosquito landings were observed during two mock 15 min human-landing catch periods at both human-landing catch positions in the semi-field cage.

### Host-Seeking Assays with Mice

Assays were performed in small (30 cm × 30 cm × 30 cm; DP1000, MegaView) or large (91 cm × 61 cm × 61 cm; BioQuip Products) screened mosquito cages. For each trial, an equal mix of 20 each wild-type and $Gr3^{ECFP/ECFP}$ females was released and acclimated for 5 min. After this period, a single female BALB/c mouse (Harlan Laboratories) anaesthetized with ketamine:xylazine was introduced into the center of the cage, and mosquitoes were given the opportunity to blood-feed for 10 min. The number of mosquitoes of each genotype that blood-fed on the mouse was scored post hoc by *ECFP* fluorescence with a Nikon SMZ1500 dissecting microscope fitted with a C-HGFI Intensilight Illuminator (Nikon Instruments Inc.). A separate mouse was used in each experimental replicate. Humans were not present during acclimation or feeding to eliminate human host cues.

### Membrane-Feeding Assay

A membrane-feeding assay was assembled using six custom 20 mm flanked glass jacketed membrane feeders (JHU-0804-081MS, Chemglass Life Sciences) connected in series via silicone tubing to a digital 12 l water bath (VWR International) set to 37°C. Technical details of the construction and operation of the assay are in the Extended Experimental Procedures.

### Statistical Analysis

Statistical analysis was performed using GraphPad Prism Software version 5.0b (GraphPad Software, Inc.).

## SUPPLEMENTAL INFORMATION

Supplemental Information includes Extended Experimental Procedures and can be found with this article online at http://dx.doi.org/10.1016/j.cell.2013.12.044.

## AUTHOR CONTRIBUTIONS

C.J.M. designed and carried out all the experiments in the paper except those in Figures 2 and 3, which were conducted by B.J.M. and R.A.C., respectively, with assistance from C.J.M. S.A.R. coordinated the semi-field cage trials in Figure 5. C.J.M., R.A.C., B.J.M., and L.B.V. composed the figures. C.J.M. and L.B.V. together wrote the paper.

## ACKNOWLEDGMENTS

We thank Matthew DeGennaro, Jeff Liesch, Carolyn McBride, and other members of the Vosshall Lab for helpful discussions and comments on the manuscript; Deborah Beck, Allison Goff, Emma Mullen, Jason Pitts, Laura Seeholzer, and Sarah Yeoh-Wang for expert technical assistance; Lindsay Bellani for collaborating to establish the membrane-feeding assay; and Scott Dewell for bioinformatic support. At James Cook University, Jessica Dickie, Chris Paton, and Michael Townsend provided valuable support with Australian importation, regulatory inspections, and mosquito rearing, and Mark Pearson facilitated sample processing. Zach Adelman of Virginia Tech University provided plasmids. C.J.M. was supported by a Marie-Josée and Henry Kravis Postdoctoral Fellowship and a Human Frontier Science Program Long-Term Postdoctoral Fellowship. B.J.M. is a Jane Coffin Childs Postdoctoral Fellow. L.B.V. is an Investigator of the Howard Hughes Medical Institute.

Received: October 6, 2013
Revised: December 12, 2013
Accepted: December 19, 2013
Published: February 27, 2014

## REFERENCES

Acree, F., Jr., Turner, R.B., Gouck, H.K., Beroza, M., and Smith, N. (1968). L-Lactic acid: a mosquito attractant isolated from humans. Science *161*, 1346–1347.

Anton, S., van Loon, J.J., Meijerink, J., Smid, H.M., Takken, W., and Rospars, J.P. (2003). Central projections of olfactory receptor neurons from single antennal and palpal sensilla in mosquitoes. Arthropod Struct. Dev. *32*, 319–327.

Benton, R., Vannice, K.S., Gomez-Diaz, C., and Vosshall, L.B. (2009). Variant ionotropic glutamate receptors as chemosensory receptors in *Drosophila*. Cell *136*, 149–162.

Bohbot, J., Pitts, R.J., Kwon, H.W., Rützler, M., Robertson, H.M., and Zwiebel, L.J. (2007). Molecular characterization of the *Aedes aegypti* odorant receptor gene family. Insect Mol. Biol. *16*, 525–537.

Burgess, L. (1959). Probing behavior of *Aedes aegypti* (L.) in response to heat and moisture. Nature *184*, 1968–1969.

Campbell, R. (2008). The processing of audio-visual speech: empirical and neural bases. Philos. Trans. R. Soc. Lond. B Biol. Sci. *363*, 1001–1010.

DeGennaro, M., McBride, C.S., Seeholzer, L., Nakagawa, T., Dennis, E.J., Goldman, C., Jasinskiene, N., James, A.A., and Vosshall, L.B. (2013). *orco* mutant mosquitoes lose strong preference for humans and are not repelled by volatile DEET. Nature *498*, 487–491.

Dekker, T., and Cardé, R.T. (2011). Moment-to-moment flight manoeuvres of the female yellow fever mosquito (*Aedes aegypti* L.) in response to plumes of carbon dioxide and human skin odour. J. Exp. Biol. *214*, 3480–3494.

Dekker, T., Geier, M., and Cardé, R.T. (2005). Carbon dioxide instantly sensitizes female yellow fever mosquitoes to human skin odours. J. Exp. Biol. *208*, 2963–2972.

Erdelyan, C.N., Mahood, T.H., Bader, T.S., and Whyard, S. (2012). Functional validation of the carbon dioxide receptor genes in *Aedes aegypti* mosquitoes using RNA interference. Insect Mol. Biol. *21*, 119–127.

Eiras, A.E., and Jepson, P.C. (1991). Host location by *Aedes aegypti* (Diptera: Culicidae): a wind tunnel study of chemical cues. Bull. Entomol. Res. *81*, 151–160.

Gallagher, M., Wysocki, C.J., Leyden, J.J., Spielman, A.I., Sun, X., and Preti, G. (2008). Analyses of volatile organic compounds from human skin. Br. J. Dermatol. *159*, 780–791.

Geier, M., Bosch, O.J., and Boeckh, J. (1999). Influence of odour plume structure on upwind flight of mosquitoes towards hosts. J. Exp. Biol. *202*, 1639–1648.

Gibson, G., and Torr, S.J. (1999). Visual and olfactory responses of haematophagous Diptera to host stimuli. Med. Vet. Entomol. *13*, 2–23.

Gillies, M.T. (1980). The role of carbon dioxide in host-finding by mosquitoes (Diptera: Culicidae): a review. Bull. Entomol. Res. *70*, 525–532.

Grant, A.J., Wigton, B.E., Aghajanian, J.G., and O'Connell, R.J. (1995). Electrophysiological responses of receptor neurons in mosquito maxillary palp sensilla to carbon dioxide. J. Comp. Physiol. A Neuroethol. Sens. Neural Behav. Physiol. *177*, 389–396.

Healy, T.P., and Copland, M.J. (1995). Activation of *Anopheles gambiae* mosquitoes by carbon dioxide and human breath. Med. Vet. Entomol. *9*, 331–336.

Huson, D.H., and Scornavacca, C. (2012). Dendroscope 3: an interactive tool for rooted phylogenetic trees and networks. Syst. Biol. *61*, 1061–1067.

Jones, P.L., Pask, G.M., Rinker, D.C., and Zwiebel, L.J. (2011). Functional agonism of insect odorant receptor ion channels. Proc. Natl. Acad. Sci. USA *108*, 8821–8825.

Jones, W.D., Cayirlioglu, P., Kadow, I.G., and Vosshall, L.B. (2007). Two chemosensory receptors together mediate carbon dioxide detection in *Drosophila*. Nature *445*, 86–90.

Keller, A., and Malaspina, D. (2013). Hidden consequences of olfactory dysfunction: a patient report series. BMC Ear Nose Throat Disord. *13*, 8.

Kennedy, J.S. (1940). The visual responses of flying mosquitoes. Proc. Zool. Soc. Lond. *A109*, 221–242.

Kröber, T., Kessler, S., Frei, J., Bourquin, M., and Guerin, P.M. (2010). An in vitro assay for testing mosquito repellents employing a warm body and carbon dioxide as a behavioral activator. J. Am. Mosq. Control Assoc. *26*, 381–386.

Kwon, J.Y., Dahanukar, A., Weiss, L.A., and Carlson, J.R. (2007). The molecular basis of $CO_2$ reception in *Drosophila*. Proc. Natl. Acad. Sci. USA *104*, 3574–3578.

Larsson, M.C., Domingos, A.I., Jones, W.D., Chiappe, M.E., Amrein, H., and Vosshall, L.B. (2004). *Or83b* encodes a broadly expressed odorant receptor essential for *Drosophila* olfaction. Neuron *43*, 703–714.

Lewis, H.E., Foster, A.R., Mullan, B.J., Cox, R.N., and Clark, R.P. (1969). Aerodynamics of the human microenvironment. Lancet *1*, 1273–1277.

Lu, T., Qiu, Y.T., Wang, G., Kwon, J.Y., Rutzler, M., Kwon, H.W., Pitts, R.J., van Loon, J.J., Takken, W., Carlson, J.R., and Zwiebel, L.J. (2007). Odor coding in the maxillary palp of the malaria vector mosquito *Anopheles gambiae*. Curr. Biol. *17*, 1533–1544.

Maekawa, E., Aonuma, H., Nelson, B., Yoshimura, A., Tokunaga, F., Fukumoto, S., and Kanuka, H. (2011). The role of proboscis of the malaria vector mosquito *Anopheles stephensi* in host-seeking behavior. Parasit. Vectors *4*, 10.

McIver, S.B. (1972). Fine structure of pegs on the palps of female culicine mosquitoes. Can. J. Zool. *50*, 571–576.

Pellegrino, M., Nakagawa, T., and Vosshall, L.B. (2010). Single sensillum recordings in the insects *Drosophila melanogaster* and *Anopheles gambiae*. J. Vis. Exp. *36*, 1–5.

Ritchie, S.A., Johnson, P.H., Freeman, A.J., Odell, R.G., Graham, N., Dejong, P.A., Standfield, G.W., Sale, R.W., and O'Neill, S.L. (2011). A secure semi-field system for the study of *Aedes aegypti*. PLoS Negl. Trop. Dis. *5*, e988.

Robertson, H.M., and Kent, L.B. (2009). Evolution of the gene lineage encoding the carbon dioxide receptor in insects. J. Insect Sci. *9*, 19.

Ruta, V., Datta, S.R., Vasconcelos, M.L., Freeland, J., Looger, L.L., and Axel, R. (2010). A dimorphic pheromone circuit in *Drosophila* from sensory input to descending output. Nature *468*, 686–690.

Small, D.M. (2012). Flavor is in the brain. Physiol. Behav. *107*, 540–552.

Smallegange, R.C., Verhulst, N.O., and Takken, W. (2011). Sweaty skin: an invitation to bite? Trends Parasitol. *27*, 143–148.

Snow, W.F. (1970). The effect of a reduction in expired carbon dioxide on the attractiveness of human subjects to mosquitoes. Bull. Entomol. Res. *60*, 43–48.

Spitzen, J., Spoor, C.W., Grieco, F., ter Braak, C., Beeuwkes, J., van Brugge, S.P., Kranenbarg, S., Noldus, L.P., van Leeuwen, J.L., and Takken, W. (2013). A 3D analysis of flight behavior of *Anopheles gambiae* sensu stricto malaria mosquitoes in response to human odor and heat. PLoS ONE *8*, e62995.

Tauxe, G.M., MacWilliam, D., Boyle, S.M., Guda, T., and Ray, A. (2013). Targeting a dual detector of skin and $CO_2$ to modify mosquito host seeking. Cell *155*, 1365–1379.

Trpis, M., McClelland, G.A.H., Gillett, J.D., Teesdale, C., and Rao, T.R. (1973). Diel periodicity in the landing of *Aedes aegypti* on man. Bull. World Health Organ. *48*, 623–629.

Turner, S.L., Li, N., Guda, T., Githure, J., Cardé, R.T., and Ray, A. (2011). Ultra-prolonged activation of $CO_2$-sensing neurons disorients mosquitoes. Nature *474*, 87–91.

Woke, P.A. (1937). Cold-blooded vertebrates as hosts for *Aedes aegypti*. Linn. J Parasitol *23*, 310–311.

## EXTENDED EXPERIMENTAL PROCEDURES

### ZFN-Mediated Targeted Mutagenesis of *AaegGr3*

#### *ZFN Design*

Prior to ZFN design, the coding sequence and exon content of *AaegGr3* (Vectorbase Accession number AAEL010058) was verified in the recipient *Orlando* strain with 3′RACE on maxillary palp cDNA. The following primers were used 5′-ATGAATCTCAACCAA GACCC-3′ and 5′-GCGAGCTCCGCGGCCGCGTTTTTTTTTTTTTTT-3′ with AccuPrime HF *Taq* polymerase (Invitrogen). For genomic PCR across the *Gr3* locus the following primers were used: (1) 5′-AGGGCATTGTTAGCGGGCATATGAA-3′ and 5′-GGTTTGT GCATCCGAGTTCATCCAA-3′ and (2) 5′-TTGGATTTCCGCCAATCTCTTCGAG-3′ and 5′- ATCGTTGCCAAAAGCTGGAATGGAA-3′ with Novagen KOD polymerase (EMD Millipore). The resulting PCR products were cloned using pCR4-TOPO (Invitrogen) and Sanger sequenced (Genewiz) to develop a consensus *Gr3* sequence. Of 16 candidate ZFN pairs predicted in silico to bind and cleave within conserved regions of nucleotide sequence across exons 1, 2, and 3 of *Gr3*, one ZFN pair (*Gr3* PZFN1/PZFN2) targeting exon 3 was chosen for use. This pair exhibited the highest levels of in vitro activity (106.7%) relative to the *CCR5* control ZFN pair in a yeast-based *MEL1* validation screen (Doyon et al., 2008) of all candidates. The nucleotide sequence of the ZFN-binding sites and nonspecific 5 nucleotide cut site for wild-type heterodimeric Fok1 endonuclease for *Gr3* PZFN1/PZFN2 are denoted in upper case and lower case letters, respectively: 5′-ATCGTTAACATCCTGCCGgttctGATCATTCCGTTGATGTG-3′.

#### *Nonhomologous End-Joining Deletion Mutants*

To generate deletion alleles, *Gr3* PZFN1/PZFN2 mRNAs (400 ng/μl) were microinjected into 550 pre-blastoderm stage *Orlando Ae. aegypti* embryos by Genetic Services Inc. Post-injection, 54 G0 larvae (9.8%) hatched, yielding 8 female and 8 male fertile G0 adults (from 31 adults total) that were outcrossed individually to wild-type *Orlando* mosquitoes to generate 16 G1 lines. PCR-based barcoding of amplicons crossing the target ZFN site coupled with Illumina sequencing was used to identify G1 pools containing mutant progeny as previously described (DeGennaro et al., 2013) with modifications. For this selection strategy, G1 progeny within each G0 progenitor line were self-crossed, blood-fed, and eggs collected en masse, before all adults from an individual G1 family were sacrificed and DNA extracted as a pool using the DNeasy protocol (QIAGEN). 16 G1 DNA pools were derived from 981 G1 adults total. Subsequently, a 388 bp gene-specific amplicon spanning the *Gr3* ZFN cut site was amplified from each DNA pool by AccuPrime HF *Taq* polymerase (Invitrogen) using *Gr3*-specific primers (bold) with Illumina adapters and 6 nucleotide barcodes (nnnnnn): 5′-AATGATACGGCGACCACCGAGATCTACACTCTTTCCCTACACGACGCTCTTCCGATCTnnnnnn**TTCGAAGAGGCCG TCATCGCTTA**-3′ and 5′-CAAGCAGAAGACGGCATACGAGCTCTTCCGATCT**TCAAAGCCCTTTGGAAATCCTCC**-3′ (total amplicon size = 486 bp). *Gr3* amplicons from each G1 pool were barcoded twice in separate PCR reactions using sets of barcodes: (PCR reaction 1) cgtgat, acatcg, gcctaa, tggtca (PCR reaction 2) cactgt, attggc, gatctg, tcaagt; such that mutant sequences could be assigned to a specific pool by the binary combination of two unique barcodes in a 4 × 4 matrix of 16 G1 families total. Barcoded PCR amplicons from each G1 pool were combined in equimolar ratios and sequenced using 100 bp single reads on an Illumina HiSeq 2000 sequencer (Rockefeller University Genomics Resource Center), and data filtered and analyzed as previously described (DeGennaro et al., 2013). In this case, 7 out of the 16 G0 lines (43.8%) passed deletion alleles to their G1 progeny

Mutant alleles identified during Illumina sequencing were isolated using size-based genotyping of single-pair crosses between progeny derived from candidate G1 pools containing the mutations and wild-type mosquitoes. *Gr3* amplicons for size-based genotyping were amplified using fluorescently labeled primers 5′-6FAM-TTCGAAGAGGCCGTCATCGCTTA-3′ and 5′-TCAAAG CCCTTTGGAAATCCTCC-3′ with AccuPrime HF *Taq* polymerase (Invitrogen), and analyzed by capillary gel electrophoresis using an Applied Biosystems 3730 DNA analyzer (Genewiz). PCR amplicons containing the deletions were cloned and Sanger sequenced to confirm mutations, and the alleles named for the number of deleted bases. After isolation, the $Gr3^{4}$ allele was outcrossed to wild-type mosquitoes for five successive generations, using size-based genotyping to select for mutant alleles at each generation before homozygotes were generated. The 4 bp frameshift in $Gr3^{4}$ alters an amino acid residue at position 150 in the 445 amino acid wild-type peptide sequence from P to F, and results in a premature stop directly after this residue. To verify that the genomic deletion led to the expected mutant transcript, mRNA was extracted from head tissue of wild-type and $Gr3^{4}$ mutant mosquitoes using RNeasy and Oligotex mRNA mini kits (QIAGEN), reverse transcribed using Superscript III Reverse Transcriptase (Invitrogen). A 555 bp amplicon (551 bp in mutants) spanning *Gr3* Exon 2 and 3 was amplified with AccuPrime HF *Taq* polymerase (Invitrogen) using the primers 5′-GATATAGTTTACGGCACCACGA-3′ and 5′-ACTGAGAGTTTCGCAGGTCATA-3′. This amplicon was subcloned into pCR4-TOPO (Invitrogen) and then Sanger sequenced (Genewiz). The sequence confirmed the proper splicing of exon 2 to 3, the presence of the 4 bp deletion, and the creation of premature stop codons caused by this frameshift.

#### *Homologous Recombination Mutants*

To facilitate ZFN-mediated homologous recombination in *Ae. aegypti*, a donor plasmid pSL1180-HR-*PUbECFP* (Addgene plasmid #47917) was made containing a fluorescent cassette flanked on either side by multiple restriction sites for inserting homologous arms. The fluorescent cassette consisted of the *Ae. aegypti polyubiquitin* (*PUb*) promoter (Anderson et al., 2010) sourced from *pMos-3xP3DsRed-PUb-EGFP-attP* (a kind gift of Zach Adelman) driving a single nuclear copy of *ECFP* with a *SV40* polyadenylation signal. To target *Gr3* using ZFN-mediated homologous recombination, homologous arms 800 bp in length flanking the *Gr3* PZFN1/PZFN2 cut site were amplified with Novagen KOD polymerase (EMD Millipore) from two genomic DNA clones tiling the *Gr3* locus using the primers: 5′-atatatgcggccgcGACGATGATGCGTTAAATATTCATCGGA-3′ and 5′-atatatgatatcCGATGAAGAGATAAGCG

ATGACGGCCTC-3′ for the left arm; and 5′-atatatggatccTGTGGTACGAAACTCGTAAGGTCTCCAG-3′ and 5′-atatatggatccAT TATTTGAAAACAGGATTATTCAATCT-3′ for the right arm; with underlined bases indicating restriction enzyme recognition sites added for cloning. *Gr3* PZFN1/PZFN2-binding sites were partially represented in each arm: 5′-ATCGTTAACATCCTGCCGgttctGAT CATTCCGTTGATGTG-3′, with underlined bases indicating the start of each arm. Using this design, 33 bp of the *Gr3* PZFN1/PZFN1 site in exon 3 were deleted and a 2452 bp *PUb-ECFPnls-SV40* cassette was inserted during targeting. Left and right arms were cloned directionally into the Not1/EcoRV and BamH1 sites of *pSL1180-HR-PUbECFP*, respectively, using standard techniques to generate *pSL1180-HR-PUbECFP-GR3*.

To generate homologous recombination alleles, *Gr3* PZFN1/PZFN2 mRNAs (200 ng/μl) and *pSL1180-HR-PUbECFP-GR3* (750 ng/μl) were microinjected into 1000 pre-blastoderm stage embryos. From these injections, 295 G0 larvae (29.5%) hatched, yielding 86 female and 119 male fertile G0 adults (from 247 adults total) that were outcrossed individually to wild-type *Orlando* mosquitoes to generate 205 independent G1 lines. To select for homologous recombinants, progeny of each G1 line were screened as larvae for *ECFP* fluorescence using a Nikon SMZ1500 dissecting microscope excited by a Nikon C-HGFI Intensilight Illuminator. We detected two G1 lines out of 205 screened in which a proportion of larvae in each family (11/83 and 1/187 G1 larvae, respectively in lines 1 and 2) constitutively expressed *ECFP*. Positive G1 adults derived from these larvae (6 G1 females and 3 G1 males in line 1; 1 G1 female in line 2) were individually outcrossed to wild-type mosquitoes, and eggs collected before adults were sacrificed for DNA extraction. To confirm directed insertion of the *PUb-ECFPnls-SV40* cassette into *Gr3* Exon 3 in these mosquitoes, two diagnostic PCR products were amplified with Novagen KOD polymerase (EMD Millipore) using *ECFP* (5′-ACAAGCAGAAGAACGGCAT CAAG-3′) and *SV40* (5′-CCTCCCCCTGAACCTGAAACATA-3′) forward primers anchored within the inserted cassette and a reverse primer in *Gr3* Exon 4 (5′-TCGTCTGGTATGCTGATTTGGAAC-3′) outside the boundary of the right arm; and PCR products cloned and Sanger sequenced. All 9 individuals tested from line 1 contained directed insertions into *Gr3* Exon 3, whereas no evidence for directed insertion was obtained from the single female in Line 2, which was discarded. A homologous recombination rate of 0.49% was calculated and defined as the percentage of fertile G0 individuals giving rise to directed homologous recombination events in F1 progeny, or 1/205 G0 lines.

A single mutant allele ($Gr3^{ECFP}$) from a G1 female in line 1 was chosen for further characterization, and outcrossed for eight generations to wild-type mosquitoes before homozygotes were generated. $Gr3^{ECFP}$ mutants were genotyped with Novagen KOD polymerase (EMD Millipore) using the primers 5′-CTTCGAGGAGAGTGTTCGGTTTG-3′ and 5′-ACCAAATAGGTCACCATCG TTGC-3′ anchored in *Gr3* exons 1 and 4 (labeled F and R, respectively, in Figures 1B and 1D). This PCR reaction produced a 3,713 bp amplicon in $Gr3^{ECFP}$ homozygous mutants, and a 1,294 bp amplicon in wild-type mosquitoes (Figure 1F).

## SciTrackS 3D Multi-Insect Tracking System

The system consists of a flight chamber (1.25 m L × 0.75 m W × 1.00 m H) with clear acrylic sides and front. Carbon-filtered air was continuously provided to this chamber by a pump (Quiet Pressure Pump, 79610-81, Cole-Parmer). $CO_2$ was added to this airstream when required through the use of a computer-controlled solenoid valve and a valve controller (Model 360D1X75R, NResearch Inc.) operated by a MATLAB (Mathworks) script through an analog/digital interface (model USB-1208FS, Measurement Computing Corporation). Tracking was accomplished by imaging the chamber with two offset cameras (model piA640-210 gm; Basler AG) with 1/2 4-12 mm F/1.2 IR aspherical objectives (Tamron). Lighting was provided by two banks of IR LEDs (model ISO-23-IRN-24-AL2, Metaphase Technologies). 3D position information of each visible mosquito was calculated in real-time at 200 Hz using custom-built software based on previously published algorithms (Fry et al., 2000). Tracks were further processed, filtered, and analyzed using MATLAB.

$CO_2$ activation assay: For each trial, 20 female mosquitoes were added to the flight chamber with a mechanical aspirator. After acclimation and tracking of baseline activity for 30 min, a 40 s pulse of 100% $CO_2$ was added to the airstream at a flow rate of 1,360 ml/min. This raised the concentration of $CO_2$ by 1,000 ppm above background levels, as measured in the middle of the flight chamber with a Carbocap Hand-Held $CO_2$ Meter (model GM70, Vaisala Inc.). Tracking continued for another 20 min to measure activity in response to this pulse of $CO_2$. Female mosquitoes had access to cotton balls soaked in 10% sucrose placed in a dish in the flight chamber. Data are presented as the population distance tracked in 10 s bins (Figure 2B), or as cumulative distance tracked per mosquito in the 6 min immediately following $CO_2$ addition (Figure 2C). Experiments and analysis were performed blind to genotype.

Daily locomotor activity assay: For each trial, 20 female mosquitoes were placed into the apparatus and tracked for 23 hr. White LED lights provided overhead illumination during the ''daylight'' phase of the mosquito rearing cycle (14 hr lights on: 10 hr lights off). A cotton wick soaked in 10% sucrose solution was provided in the flight chamber. Data are presented as the distance tracked per mosquito in 10 min time bins (Figure 2D), cumulative tracked distance per mosquito over the 23 hr experiment, and the mean velocity of all individual tracks (Figure 2E). Experiments and analysis were performed blind to genotype.

## Two-Port Olfactometer Assays

During each trial, 50 female mosquitoes were introduced into the central chamber of the olfactometer and allowed to acclimate to assay conditions for 10 min. Treatment odors ± $CO_2$ were then introduced into the stimulus port at the beginning of the assay, after which time mosquitoes were allowed to fly upwind into the stimulus or blank port for 8 min. The number of mosquitoes attracted to stimulus and blank trapping chambers at the cessation of this time period was then scored.

In trials where supplemental $CO_2$ was added, a 10% $CO_2$: 90% custom air mixture (GTS-Welco) was introduced into the system via Nalgene tubing placed inside the stimulus port for a final concentration of 2,000–3,000 ppm $CO_2$, as measured using a CARBOCAP Hand-Held Carbon Dioxide Meter (GM70, Vaisala Inc.). To test mosquito responses to lactic acid, we placed 4 ml L(+)-lactic acid solution (C.A.S. 79-33-4, catalog number 27714; 88%–92%; Sigma-Aldrich) into the open base of a 60 mm diameter × 15 mm height Petri dish (0875713A, Thermo Fisher Scientific) positioned at the center of the stimulus port. To test mosquito responses to human odor or live humans we placed a nylon sleeves infused with human-odor or a live human arm respectively into the stimulus port as described previously (DeGennaro et al., 2013). Supplemental $CO_2$ was not added in assays with live human arms due to pilot observations of a ceiling-like effect with high levels of attraction that was independent of whether $CO_2$ was added or not. For all treatment conditions, stimulus and blank ports were alternated between experimental replicates to control for side bias. Background responses were evaluated using blank trials with wild-type mosquitoes where no stimulus was presented in either port.

### Membrane-Feeding Assay

Two 137016 extra-large fountain pumps (Sunterra) were used to circulate water through the outer jacket of the feeders, with three feeders connected in each series to each pump. Membrane feeders from these two linked series were placed inside the central assay chamber which consisted of a translucent polypropylene storage box 36 cm L × 31 cm W × 32 cm H (The Container Store) with a removable lid. Four 1.5 cm holes made on opposite walls of the chamber allowed the exit and entry of silicone tubing connecting the feeders to pumps and water bath. A $CO_2$ diffusion pad (8.9 cm × 12.7 cm; Tritech Research) was affixed to the inner center of the lid to allow delivery of purified air and $CO_2$ to condition the chamber atmosphere when required. A plastic platform (31 cm × 26 cm) with 4 cm × 3 cm legs was inserted into the inner chamber to create an elevated false floor that containing six evenly spaced circular holes (8 cm diameter) designed to hold 6 × 16 oz paper cups (KH16A-J8000, Solo Cup Company) covered in white 0.8 mm Polyester Mosquito Netting (American Home & Habit Inc.) to house mosquitoes. Feeding positions were randomized according to genotype during assays.

Membrane feeders were prepared for use by stretching a double-layer of Parafilm M laboratory film (Bemis Company, Inc.) over the feeder reservoir, and filling them with 400 μl of heparinized whole sheep blood (Hemostat Laboratories). In experiments where human odor was required, 3.5 cm × 3.5 cm squares of sheer knee high nylon stockings (Duane Reade) previously worn continuously for 33 hr by human volunteers were affixed to membrane using a rubber band. Clean stocking was affixed to the membrane in all other experiments. During each trial, 6 cups of mosquitoes (n = 25 per cup) were introduced into their feeding positions in the central chamber, the apparatus closed, and mosquitoes allowed to acclimate to assay conditions. Charcoal-purified air was provided continuously throughout each assay via a quiet pressure pump (Part No. 2415B-01, Welch-Gardner Denver). After 5 min acclimation, fountain pumps were switched on to circulate warm water to the membrane feeders for a period of 15 min. In trials involving supplemental $CO_2$, a custom 10% $CO_2$: 90% air mixture (GTS-Welco) was added continuously to the assay atmosphere during heating at a rate of 1,592 ml/min using a Single Tube Rotameter Flow meter (P16A1-BA0A-023-92-ST, Aalborg) to increase $CO_2$ concentration to 15,000 ppm above background levels. After 15 min, cups were removed from the apparatus and mosquitoes cold anaesthetized. Blood feeding was visually scored and any mosquitoes that did not appear to have blood-fed were crushed between absorbent papers. The animal was scored as blood-fed if there was any evidence of blood on the paper.

## SUPPLEMENTAL REFERENCES


Anderson, M.A., Gross, T.L., Myles, K.M., and Adelman, Z.N. (2010). Validation of novel promoter sequences derived from two endogenous ubiquitin genes in transgenic *Aedes aegypti*. Insect Mol. Biol. *19*, 441–449.

DeGennaro, M., McBride, C.S., Seeholzer, L., Nakagawa, T., Dennis, E.J., Goldman, C., Jasinskiene, N., James, A.A., and Vosshall, L.B. (2013). *orco* mutant mosquitoes lose strong preference for humans and are not repelled by volatile DEET. Nature *498*, 487–491.

Doyon, Y., McCammon, J.M., Miller, J.C., Faraji, F., Ngo, C., Katibah, G.E., Amora, R., Hocking, T.D., Zhang, L., Rebar, E.J., et al. (2008). Heritable targeted gene disruption in zebrafish using designed zinc-finger nucleases. Nat. Biotechnol. *26*, 702–708.

Fry, S.N., Bichsel, M., Müller, P., and Robert, D. (2000). Tracking of flying insects using pan-tilt cameras. J. Neurosci. Methods *101*, 59–67.